mm-CUR: A Novel Ubiquitous, Contact-free, and Location-aware Counterfeit Currency Detection in Bundles Using Millimeter-Wave Sensor

FAHIM NIAZ, School of Computer Science, Wuhan University, China
JIAN ZHANG*, School of Computer Science, Wuhan University, China
YANG ZHENG, School of Computer Science, Wuhan University, China
MUHAMMAD KHALID, School of Computer Science, University of Hull, UK
ASHFAQ NIAZ, College of Electrical and Power Engineering, Taiyuan University of Technology, China

Abstract: Target material sensing in non-invasive and ubiquitous contexts plays an important role in various applications. Recently, a few wireless sensing systems have been proposed for material identification. In this paper, we introduce mm-CUR, A Novel Ubiquitous, Contact-free, and Location-aware Counterfeit Currency Detection in Bundles using a Millimeter-Wave Sensor. This system eliminates the need for individual note inspection and pinpoints the location of counterfeit notes within the bundle. We use Frequency Modulated Continuous Wave (FMCW) radar sensors to classify different counterfeit currency bundles on a tabletop setup. To extract informative features for currency detection from FMCW signals, we construct a Radio Frequency Snapshot (RFS) and build signal scalogram representations that capture the distinct patterns of currency received from different currency bundles. We refine the RFS by eliminating multi-path interference, and noise cancellation and apply high pass filters for mitigating the smearing effect with the continuous wavelet transform (CWT). To broaden the usage of mm-CUR, we built a transferable learning model that yields robust detection results in different scenarios. The classification results demonstrated that the proposed counterfeit currency detection system can detect counterfeit notes in 100-note bundles with an accuracy greater than 93%. Compared to the standard CNN and DNN methods, the proposed mm-CUR model showed superior performance in distinguishing each bundle data, even for a limited-size dataset.

CCS Concepts: • **Ubiquitous and mobile computing → Ubiquitous and mobile putting systems and tools, Contact-free sensing**.

Additional Key Words and Phrases: mmWave Sensor, Counterfeit Currency, Currency Detection, Wireless Sensing, Contact-free Sensing

1 Introduction

While electronic financial transactions are gaining popularity and the usage of physical currency is declining, banknotes remain in circulation due to their reliability and user-friendly nature. Consequently, the challenges associated with automated banknote processing remain pertinent. These challenges encompass tasks like identifying banknote types and denominations, detecting counterfeit bills, categorizing fitness, and recognizing serial numbers. These tasks are predominantly executed in automated transaction facilities like counting machines or vending machines, employing image processing techniques [1]. Among these tasks, counterfeit detection assumes an essential role in ensuring transaction security, given the persistence of sophisticated fake notes. Current anti-counterfeit measures applied to

*Corresponding Author

Authors' addresses: Fahim Niaz, notify.fahim@outlook.com, School of Computer Science, Wuhan University, Wuhan, China; Jian Zhang, jzhang@whu.edu.cn, School of Computer Science, Wuhan University, Wuhan, China; Yang Zheng, zh.yang@whu.edu.cn, School of Computer Science, Wuhan University, Wuhan, China; Muhammad Khalid, M.Khalid@hull.ac.uk, School of Computer Science, University of Hull, Hull, UK; Ashfaq Niaz, ashfaq123niaz@gmail.com, College of Electrical and Power Engineering, Taiyuan University of Technology, Taiyuan, China.

2024. Manuscript submitted to ACM

banknotes include features like security threads, anti-copy patterns, watermarks, and hologram patterns. However, the frequent verification of counterfeit notes is hindered by the substantial number of notes in circulation and the intricate nature of detection methods, encompassing various sensors like magnetic, infrared (IR), or ultra-violet (UV) sensors. Consequently, the general public finds it challenging to identify counterfeit banknotes.

Smart sensing technologies have become essential in non-invasive sensing and identifying a wide range of objects and materials [2]. The key factor behind its significance is its role in ensuring contamination and infection control, as well as preventing accidents. Furthermore, these technologies play a crucial role in reducing environmental disruption by identifying dangerous objects or materials. Among the leading techniques [3] for non-invasive material detection are X-ray diffraction [4], and X-ray fluorescence [5], [6]. Both methods excel in their ability to analyze materials qualitatively and quantitatively. However, it's worth noting that X-rays are a form of ionizing radiation. Prolong exposure can pose health risks to both the subject being examined and the operator. While optical, infrared, and multi-spectral imaging technologies can detect reflections from a target, they often fall short when come across the penetrating the surface of non-opaque materials. Conversely, millimeter-wave (mmWave) radar sensing is gaining attraction for subsurface detection. The widespread commercial accessibility of this non-ionizing sensor holds significant potential for material identification [7]. Whether in the form of an integrated chip-set [8], [9] or a packaged module, compact mmWave radar sensors are available and reliable, streamlining the cost-effective integration of material identification in production and processing workflows. The unique properties of signals reflected from various material layers can offer distinctive signatures, thereby facilitating the identification of the given subject [10].

Contrasting current counterfeit currency detection systems, this paper delves into the potential of utilizing RF signals for ubiquitous and contact-free currency monitoring. Our objective is to deduce the authenticity of currency based on radio signals, which show unique patterns when reflected by legitimate or counterfeit notes. The system demands no alterations, making mm-CUR compatible with standard currencies available off-the-shelf. With no need for visual inspections or sensor repositioning, the system emphasizes convenience and user accessibility. However, with the aspiration to establish a ubiquitous contact-free RF-driven system to distinguish between genuine and counterfeit currency in note bundles, we face the following challenges.

- **Q1:** How we can extract information about genuine and counterfeit currency from mmWave radar signals?

Earlier studies have used RF signals for grid map construction [11], user identification [12], [13], vital sign detection [14], [15], tire wear measurement [16], medication self-administration monitoring [17], and temperature measurement [18]. mmWave radar systems offer high resolution of 30GHz to 300GHz, which means that they can detect and differentiate between small-scale objects or properties with precision. Although mmWave radar systems are known for their high resolution in various applications, such as wireless sensing and communication, their resolution can be limited when it comes to specific tasks like currency detection. This limitation arises from factors such as the wavelength used and the size of the antenna array, which impact the system's ability to resolve fine-grained features necessary for currency analysis. To address this challenge, our proposed solution focuses on enhancing the resolution and accuracy of mmWave radar signals through Radio Frequency Snapshots (RFS) enhancement. By improving the resolution capabilities in the context of currency detection, we aim to overcome the limitations posed by standard mmWave radar devices and enhance the system's ability to detect counterfeit currency effectively.

- **Q2:** How to refine and remove noise from signal RFS to generate scalograms?

The primary challenge, we faced during experiments that how we could extract precise and meaningful features to effectively differentiate between various types of currency bundles that contain counterfeit currency. These bundles consist of a varying mix of genuine and counterfeit currency notes. To overcome this issue, we employed a CWT-based noise cancellation and applied a high-pass filter to process the radar signals. However, setting the optimal cutoff frequency emerged as a complex task, necessitating a balance between preserving critical information and filtering out extraneous lower-frequency elements. Calibrating the filter for effective counterfeit detection while minimizing data loss was indeed a nuanced aspect of this research.

- **Q3:** How to extract intrinsic features from CWT-based bundle scalograms?

The third major challenge was the extraction of significant features from CWT-based scalograms. Scalogram is the graphical representation of wavelet transforms, which are rich in information, offering both time and frequency-based characteristics of the signals. However, the extraction of meaningful and discriminative features from scalograms for currency detection was a complex task. Identifying the most informative features amongst the multitude of data points in the scalogram required extensive experimentation and analysis.

In our research, we address all the challenges inherent in the design of mm-CUR, a radio frequency (RF)-driven system designed for detecting counterfeit currency. This system leverages commercially available radar technology and comprises three main components, i.e., Radio Frequency Snapshots (RFS), signal preprocessing feature extraction, and a transferable learning model. Firstly, we compute RFS for each currency bundle based on the reflected Frequency Modulated Continuous Wave (FMCW) signals under the radar from the top of the table. In the second step, we leverage the Continuous Wavelet Transform (CWT) to remove the multi-path interference and noise from the raw RFS. Radar signals are highly discriminative and have distinct characteristics. To normalize these variations, we compute the average of five RFS and subsequently generate a scalogram for each averaged RFS. Finally, for the transferable learning model, we design a Heuristic Domain Adaptation network [19] architecture with a carefully designed training dataset segmentation strategy. Comprehensive testing was carried out using various parameters. The experimental findings affirm that mm-CUR consistently attains a detection precision exceeding 93%. Furthermore, it was evident that mm-CUR is capable of acclimating to novel environments, solidifying its potential for counterfeit currency detection deployment.

We outline our principal contributions as follows:

- To the best of our knowledge, this is the pioneering effort to explore the potential of utilizing mmWave RF signals for counterfeit currency detection, and realize a ubiquitous, contact-free, and convenient location-based counterfeit currency detection system for note bundles.
- We design a suite of advanced algorithms to extract meaningful data patterns from the RF signal snapshots and have enhanced the methodology behind scalogram creation.
- We implement and assess mm-CUR in practical scenarios through rigorous testing. Our findings indicate that mm-CUR excels at identifying counterfeit currency within note bundles with high precision.

2 Related Work

Banknotes often incorporate various anti-counterfeiting features that become apparent under specific light wavelengths to facilitate counterfeit detection. Prior studies on counterfeit banknote detection have leveraged either single sensors or combinations thereof to record the optical attributes of examined banknotes. The work in [20] utilized RGB color and UV data to detect counterfeit currency. Their method integrated a detection algorithm founded on low-resolution multi-spectral images comprising RGB images from both sides and IR images across three frequencies. The multi-spectral images in conjunction with linear and quadratic classifiers for resource-constrained devices were proposed in [21]. This technique followed a similar multi-spectral image acquisition method. In [22], a neural networks model is proposed to detect counterfeit currency, the parallel piped classification approach is used for counterfeit detection. Conversely, [23] introduced a combined approach for banknote recognition and counterfeit detection. Their methodology hinged on a convolutional neural network (CNN) classifier that processed aligned visible light, IR reflection, and IR transmission images of banknotes. When focusing on single-sensor studies, there's an expansive range of wavelengths used to image banknotes, spanning IR [24], visible light [25], [26], and UV [27]. Most non-visible light studies primarily aimed to capture security features, such as latent patterns via UV light, or contrasting areas on Euro banknotes under IR. X-rays have also been harnessed for both counterfeit notes [28], [29], and banknote pigment-based counterfeit detection [11]. Given the fixed positioning of security features on banknotes, many of these detection methods presupposed knowledge of banknote denomination and insertion direction or necessitated prior banknote type recognition. Visible-light-based techniques predominantly relied on banknote color characteristics for counterfeit detection. For instance, [26] applied the luminance histogram of the Y channel in the YIQ color space of a scanned banknote for detection purposes. Similarly, [27] captured images of banknotes placed on a backlight panel using a webcam. In both instances, the support vector machine (SVM) served as the classifier.

The integration of communication and radar systems [30], [31] has gained traction as it harnesses both spectral and hardware assets to allow dual functionalities within a unified system. This paves the way for a novel approach to maximizing the use of the restricted RF spectrum [32]. The [33] proposed E-Eye to develop an economical and practical technique for recognizing hidden electronic devices. This method aims to facilitate efficient screenings to mitigate the risks posed by concealed electronic devices in everyday settings. Notably, the mmWave domain is emerging as a sought-after solution for short-range, high-capacity communication, and it also holds potential for radar sensing applications [34]. When it comes to material identification, mainstream and commercial platforms often turn to methods like optical spectroscopy, expansive radar setups, X-rays, and CT/MRI. While these yield detailed outcomes, they demand specialized, hefty, and expensive equipment, constraining their usage primarily to labs and crucial security contexts. The push for material identification in more versatile environments has grown in recent times [35], [36], [37]. The advent of compact radar sensors, such as Soli, has paved the way for radar-driven precision motion sensing, which finds applications in human-computer interaction [38]. For instance, the integration of micro-gestures detected by Soli with larger gestures fosters an intuitive input method in gesture-oriented Augmented Reality platforms. Compared to other gesture-sensing technologies, these sensors offer a compact design, energy efficiency, and enhanced privacy. Their versatility allows them to be seamlessly incorporated into daily-use consumer products like Google's Pixel 4 smartphone and the Nest Hub smart display. Moreover, the realm of radar is not limited to gesture detection; it also encompasses material and object identification.

FG Liquid [39] employs radar to differentiate between liquids up to 40cm, albeit with the limitation of a static distance for objects. Cube sense [40], while supporting radar interactions based on corner reflectors, falls short in distinguishing between various corner reflectors and objects. [38] showcased the capability to sense and categorize objects placed directly on the radar sensor, catering to context-aware and tangible applications. Yet, it's worth noting that their system's material differentiation relies on a consistent distance to the sensor and alterations in material attributes. A noteworthy contribution comes [41] which utilized a microwave Doppler sensor array positioned beneath a table. FerroTag [42] a paper-based, mmWave-scannable tagging infrastructure for next-generation inventory management systems. it is ultra-low cost, environmentally friendly, battery-free, and capable of in-situ processing, meaning multiple tags can be simultaneously scanned even when not in the line of sight. In [43], put forth an innovative low-cost approach, introducing tangible controllers based on origami structures paired with mmWave radar sensors. However, a clear identification methodology for these controllers remained unexplored.

Different from all existing systems, mm-CUR achieves the detection of counterfeit notes within note bundles without individually examining each note, leveraging RF signals. We meticulously capture RF snapshots, drawing out signal attributes from the reflected signals through enhanced scalograms that highlight discrepancies between genuine and counterfeit currency bundles. Furthermore, we developed a transferable learning model that expands the usage of mm-CUR to other currencies. Compared with existing counterfeit-detecting systems, mm-CUR is contactless, ubiquitous, and user-friendly.

3 Preliminaries

In this section, we explore the motivations for using mmWave radar technology for counterfeit currency detection, elucidating why we chose this approach. Also, We discuss the distinguishing features between genuine and counterfeit currency and introduce the concept of Radio Frequency Snapshots (RFS).

3.1 Motivation

The use of mmWave radars for material sensing in everyday contexts offers numerous applications. For instance, it can greatly improve household waste sorting, a common sustainability practice in many countries. This technology is especially useful because it can distinguish between materials that often look similar, making the sorting process more efficient and accurate. Additionally, material sensing through mmWave radars can enhance home security by detecting water leakage and enable microwave ovens to identify and alert users about the presence of metals. Metal detection also proves advantageous in tasks such as inspecting suspicious objects [19] and supporting autonomous drones [44].

The motivation behind the development and implementation of the mm-CUR model stems from the shortcomings of existing counterfeit currency identification methods. Counterfeit currency identification often relies on centralized authorities utilizing specialized machines and techniques, such as acid-free paper, optically variable ink, fine-grained marks, plastic-paper integration, UV/IR marks, and holograms. While these security features are effective, they can be challenging for civilians to verify without access to specific low-cost tools or knowledge. Although there are accessible methods like iodine ink pens and optically variable ink tests available to the public, these require manual inspection and are often limited to detecting individual notes, making the identification of fraudulent currency notes less efficient and potentially less accurate when dealing with larger quantities. The existing methods of counterfeit currency detection often rely on individual inspection of each banknote within a bundle. While these methods can be effective to some extent, they are time-consuming and labor-intensive, which makes them prone to human error and inefficiencies. Furthermore, these methods often require low-cost tools to identify whether an authentic mark is present or not, and these tools are typically not readily available to the public. This lack of accessibility and transparency in counterfeit currency detection has created a need for alternative, accessible, and efficient technologies that can empower the public to detect counterfeit currency independently. In contrast, mm-CUR approach based on mmWave offers several unique advantages:

Non-Invasive Detection: Unlike traditional methods that require direct interaction with the note (e.g., applying ink or physically manipulating the note), mm-CUR can scan bundles of notes non-invasively and without requiring manual handling, reducing the risk of damage or alteration.

Bulk Analysis Capability: This technology can analyze an entire bundle of currency notes at once, detecting not only the presence of counterfeit notes but also their exact locations within the bundle. This greatly increases the efficiency of the detection process compared to manual inspection methods.

-Material-Independence: It detects counterfeit notes based on their unique electromagnetic signatures, which are less likely to be successfully replicated by counterfeiters. This makes the detection process less dependent on the specific materials or inks used, which could be faked or degraded over time.

Integration with Everyday Devices: The potential to integrate mmWave radar technology into everyday devices, such as smartphones, further enhances accessibility and convenience, providing a portable and user-friendly solution for civilians.

Nonetheless, compared to existing signatures, the mmWave signature represents a new mechanism with unique advantages. These benefits make mmCUR a valuable complement to existing counterfeit detection technologies, offering a more comprehensive, efficient, and accessible solution for detecting counterfeit currency.

3.2 Why mmWave Radar

In recent years, there has been a significant rise in wireless sensing [45], [46], [47], [48], [49], [50], [51] where radar-like features reused radio signals originally intended for indoor communication. Moreover, dedicated radar systems are gaining popularity for both indoor and mobile applications. Notably, Apple and Google have incorporated UWB radar and mmWave radar into their latest phone models. Another notable research trend is the joint design of communication and radar systems that leverage the same hardware and spectral resources for dual functionality [32], [52]. The utilization of mmWave radars, equipped with large bandwidth and phased antenna arrays, holds promise for such integrated systems [53]. Commodity routers already offer WiFi, standardized as 802.11ad/ay, and this technology is being integrated into smartphones and vehicles [54]. The industry is actively exploring mmWave radar capabilities by re-purposing these mmWave radios. For instance, the device used in our work is a TI IWR1443 [55] product that offers a radar-like mode on top of a commodity 77-81GHz networking chip. This radar device presents distinct advantages as it leverages the existing networking infrastructure and can seamlessly transition into a ubiquitous radar system. Notably, it offers superior signal quality for wireless sensing compared to the 2.4GHz/5GHz WiFi [56]. The utilization of mmWave radar for counterfeit currency detection in note bundles is driven by several key reasons. Firstly, mmWave radar could differentiate between different materials based on their distinct electromagnetic signatures. This capability is crucial in distinguishing genuine banknotes from counterfeit ones, as counterfeit notes often exhibit different material properties. Secondly, mmWave radar enables non-contact sensing, allowing for efficient and non-destructive examination of banknotes within bundles or stacks. It can penetrate through materials and analyze the reflected signals, making it possible to detect hidden or concealed objects within banknote bundles, such as security threads or other counterfeit indicators. Additionally, mmWave radar systems offer high resolution and accuracy, enabling the identification of subtle differences between genuine and counterfeit banknotes that involve intricate design elements or security features. Lastly, with the increasing availability of mmWave radar technology, including integration into smartphones and other devices, it becomes feasible to deploy counterfeit currency detection capabilities ubiquitously. This means that individuals can utilize their everyday devices for quick and reliable counterfeit detection, enhancing overall security.

3.3 Comparison of Existing Counterfeit Currency Detection Systems with mmWave Sensors

Existing counterfeit detection systems utilize various technologies, each with specialized machines with their methods. However, these technologies often have cost, size, and effectiveness limitations, and they are generally not accessible to the public. As shown in Table 1, Infrared (IR) detection machines, such as the AccuBANKER AB5000 IR [57] currency detector, use IR sensors to reveal unique features on banknotes by capturing and comparing IR light reflections. While accurate, these machines can be expensive and bulky, making them less suitable for small businesses and individuals. Visual inspection tools vary widely, from magnifying microscopes like the Carson MicroBrite Plus to advanced automated machines such as the Glory UW-500 [58], which utilize high-resolution cameras to detect security features. Manual tools are affordable but can be time-consuming and susceptible to human error. On the other hand, automated systems offer efficiency but are costly and require substantial space. Ultraviolet (UV) detection machines, like the Cassida 5520 UV/MG Money Counter [59], use UV light to reveal fluorescent patterns on banknotes. Although relatively affordable, these machines are limited to detecting UV-reactive features and can be circumvented by sophisticated counterfeiting methods. Magnetic detection machines, such as the Safescan 185-S and G-Star Technology Money Counter, scan for magnetic properties in inks or metallic threads embedded within the currency. While these machines are fast and automated, they are restricted to currencies with magnetic features and can be quite expensive.

Table 1. Comparison of Commercial Off-The-Shelf (COTS) Devices, Typically used for Detecting Counterfeit Currency, with mmWave Radar

Class	**Device**	**Detection Properties**	**Detection Type**	**Availability**	**Location Based**	**Price**	**Ref.**
Infrared (IR) detection	AccuBANKER AB5000 IR	Unique Features IR Light Reflections	Single Note	Businesses Offices Banks	✗	\$500	[57]
Visual inspection	Glory UW-500	Watermarks Holograms Micro-Printing	Single Note	Businesses Offices	✗	\$65,000	[58]
Ultraviolet (UV) detection	Cassida 5520 UV/MG	Fluorescent Patterns Magnetic Properties Ink	Single Note	Banks	✗	\$400	[59]
mmWave Sensor	**TI-IWR1443**	**Watermarks Note Material Holographic Elements**	**Single/Bundle Note**	**Individual Users Businesses Banks**	✓	**\$200**	[60]

In contrast to traditional methods, mmWave radar technology offers significant advantages. mmWave sensors [60] are cost-effective, widely available, and can be integrated into smartphones, making them accessible to individual users. Machines equipped with mmWave radar utilize mmWave frequencies to penetrate currency bundles and detect anomalies, offering high accuracy and the ability to locate counterfeit notes within a bundle. This technology enables the detection of counterfeit notes without the need to inspect each note individually, making the process highly efficient in terms of both time and cost. The non-invasive and rapid nature of mmWave radar systems makes them a promising alternative for modern counterfeit detection, suitable for both institutional and personal use.

3.4 Genuine and Counterfeit Currency Features

Banknotes incorporate various security features to deter counterfeiting attempts. These include note material such as polymer or cotton, watermarks that are visible under light, invisible marks detectable under specific lighting conditions, holograms for authentication, and micro-text requiring high magnification to read. Moreover, Genuine currency [61] is typically printed on high-quality, acid-free paper. This special paper is designed to endure long periods without degrading, which is essential for maintaining the physical integrity of money as it circulates over time. Genuine currency exhibits consistent and well-defined features across these elements, showcasing high-quality material composition, clear and intact watermarks, accurately reproduced invisible marks, authentic holograms with no anomalies, and precise micro text legibility. Counterfeit currency often uses inferior materials that may include acid-containing papers because these are more readily available and less expensive than the specialized acid-free paper used in genuine currency.

For our experiments, we used acidic, printed, and locally made counterfeit currency notes, the main properties used for detection are paper material, watermarks, and holographic elements, which exhibit specific patterns in genuine currency. Counterfeit currency often exhibits deviations in these features compared to genuine notes, such as inconsistencies in material composition, altered watermarks, missing invisible marks, discrepancies in hologram quality, and inaccuracies in micro-text reproduction. Leveraging radar technology, our system can effectively detect these counterfeit features, as well as identify the consistent features present in genuine currency. Radar enables precise analysis of material properties, identification of hidden marks, authentication of holographic elements, and verification of micro text integrity. By correlating radar data with known security features of genuine currency, our system accurately differentiates between genuine and counterfeit currency, providing a robust solution for currency authentication and fraud prevention.

3.5 Radio-Frequency snapshots (RFS)

The biggest challenge in using commodity radar to detect genuine and counterfeit currency is how to extract useful features from the radar signal that can be used to detect counterfeit currency. Most of the existing research uses radar frequency-modulated continuous wave (FMCW) to detect derived movements and ranges [62], [16] which is not suitable for currency detection. Nevertheless, we have examined that radar signals reflected by genuine and counterfeit currency show different patterns. To characterize this discrimination, we took RFS from the reflected radar signal. This can be used to indicate the difference in genuine and counterfeit currency bundles.

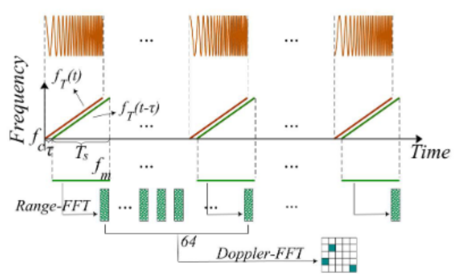

Fig. 1. Radio Frequency Snapshot (RFS).

As shown in Fig. 1, the process of Radio Frequency Snapshot (RFS). At the top, you can observe the signal in the time domain, the transmitted signal is denoted as $f_T(t)$, while $f_T(t-\tau)$ represents the reflected signal. f_m corresponds to $S_{M1}(t)$ which is discussed below. Additionally, f_c denotes the start frequency, B stands for the sweep bandwidth, T_s represents the sweep time, and τ indicates the time delay of the reflected signal. The transmitted chirp frequency of the signal increases linearly with time, and it is denoted by

$$f_T(t) = f_c + \frac{B_s}{T_s}t \tag{1}$$

where B_s is the sweep bandwidth, t is the time, f_c is the starting frequency, and the sweep time is T_s. The signal phase of the transmitted chirp is

$$p(t) = \int_0^t f(t')dt' = 2\pi \left(f_c t + \frac{B_s t^2}{2T_s} \right) \tag{2}$$

The transmitted signal can be expressed as:

$$R_T(t) = \cos\left(2\pi \left(f_c t + \frac{B_s t^2}{2T_s} \right)\right) \tag{3}$$

where cos represents the cosine function, and the slope of the sweep is denoted by B_s and T_s. The amplitude of the expected sweep signal is 1, and the received signal is given by:

$$R_R(t) = S_T(t-\tau) = \cos\left(2\pi \left(f_c(t-\tau) + \frac{B_s(t-\tau)^2}{2T_s} \right)\right) \tag{4}$$

where τ represents the reflected signal time delay. The signal amplitude attenuation is ignored. Multiplying the received signal with the transmitted signal, we get:

$$S_{M1}(t) = R_R(t)S_T(t) = \frac{1}{2}\left[\cos\left(2\pi \left(f_c t + \frac{B_s t^2}{2T_s} + f_c(t-\tau) + \frac{B_s(t-\tau)^2}{2T_s} \right)\right)\right] \tag{5}$$

Filtering the high-frequency component, we obtain:

$$S_{M1}(t) = \cos\left(2\pi \left(f_c \tau - \frac{B_s(\tau^2 - 2t\tau)}{2T_s} \right)\right) \tag{6}$$

To gain the full context of the reflected signal, we apply the range-FFT to $S_{M1}(t)$, represented as $S_{M2}(t) = \text{rangeFFT}(S_{M1}(t))$. α_t is the duration of the chirp signal. We create an RFS using a series of chirps:

$$RFS(t) = \text{dopplerFFT}(S_{M2}(t_1, t_2, \ldots, t_{64})) \tag{7}$$

where $S_{M2}(t_1, t_2, \ldots, t_{64})$ denotes a time series of $S_{M2}(t)$. The time duration of one RFS is $\alpha_t \times N$ ms, where α_t is the duration of the chirp.

4 mm-CUR Model Overview

4.1 Overview

This research paper presents an innovative, ubiquitous, contactless, and location-based method to detect counterfeit currency within a bundle of notes, eliminating the need to individually inspect each note utilizing mmWave radar technology. As shown in Fig. 2, this methodology involves three main components: data collection, RFS preprocessing feature extraction, and a ResNet-50 transferable learning model. Initially, Fig. 3a shows the data collection from the tabletop radar setup at 0.05-0.45 meters (5cm-45cm). The raw mmWave signals are segmented into equal RFS and processed through several steps: detrending to remove linear trends, noise reduction, and multi-path interference mitigation using the Daubechies wavelet (db1), and applying a high-pass filter to highlight high-frequency components. The processed RFS is transformed using continuous wavelet transform (CWT) to generate a scalogram of each RFS. It is a visual representation of how the signal's frequency content changes over time, and highlights unique patterns or anomalies related to counterfeit currency notes present in the bundle, also enhancing the counterfeit detection system's accuracy and reliability. Finally, we create a transfer learning model that can identify and detect genuine and counterfeit currency in the notes bundle for the existing and new environments. We derive intrinsic characteristics of samples from the source and the target domain. By quantifying the distinctions between these domain samples, we aim to reduce the transfer variance, subsequently isolating domain-centric details from the intrinsic data obtained. Ultimately, the mm-CUR model adeptly differentiates between genuine and counterfeit notes within the note bundles.

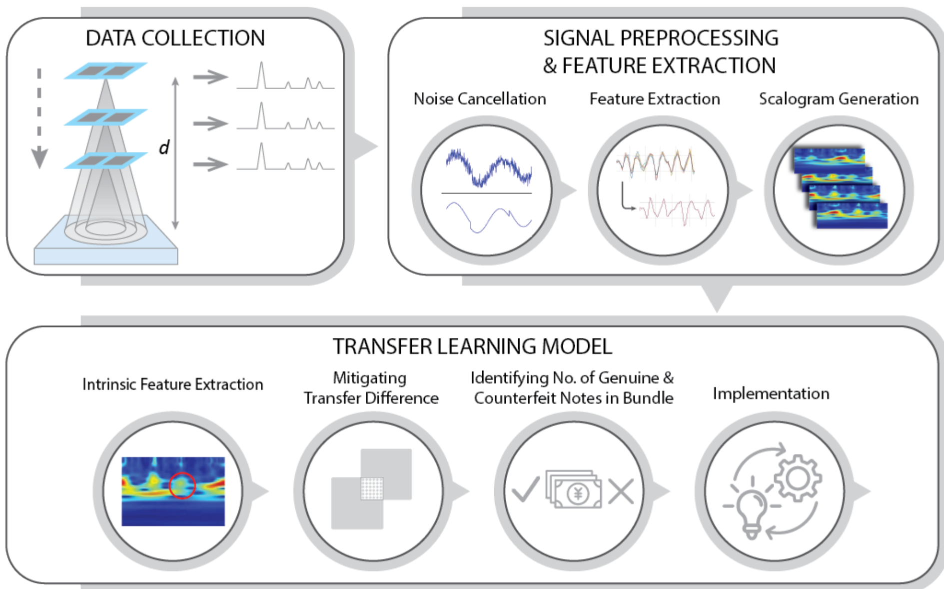

Fig. 2. mm-CUR Model Overview

4.2 Data Collection

We employ a commercial off-the-shelf (COTS) mmWave radar [55] for RF signal transmission and reflection. Complementing this, a COTS DCA1000EVM [60] is utilized for 1-Gbps Ethernet data streaming directed to a computer, as depicted in Fig. 3a and Fig. 3b. The radar operates within a frequency range of 77 to 81 GHz, corresponding to a transmitted signal wavelength of 4 mm. It consists of three collocated transmitting antennas and four receiving antennas. The radar's field of view spans 120 degrees horizontally and 30 degrees vertically. Each Frequency Modulated Continuous Wave (FMCW) chirp consists of 256 ADC samples with a set slope of 29.982MHz/us.

The data collection process is a meticulous task designed to ensure a broad spectrum of genuine and counterfeit currency instances. The foundation of this dataset lies in both genuine and counterfeit banknotes, which we source directly from a local bank. To add diversity and emulate realistic scenarios, we adopt a strategic process of inserting counterfeit notes into bundles of genuine currency. We start by inserting a single counterfeit note into the bundle, adjusting its position throughout the bundle, and capturing radar signals at each position. This method is iterated with one to twenty counterfeit notes placed at various possible locations within the bundle, each time recording the radar signal. In addition to these combinations, we also record radar signals from bundles devoid of any counterfeit notes, representing entirely genuine bundles. Conversely, we also collect data from bundles composed entirely of counterfeit notes. This allows our model to learn the range of signals from entirely genuine to entirely counterfeit scenarios. We

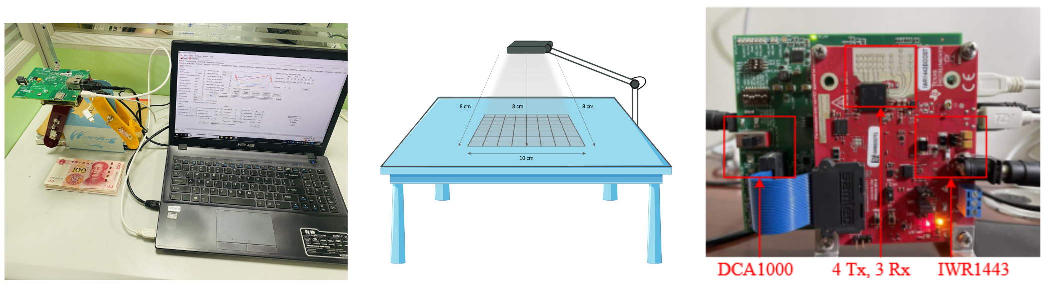

(a) (b) (c)

Fig. 3. (a), (b), and (c) Illustrate the Process of Radio-Frequency Snapshot (RFS) Collection and mmWave Radar.

collected radar signals from 21 currency bundles for genuine and counterfeit sample collection, radar signals were acquired from 21 currency bundles. Each bundle represents a specific configuration: bundle_1 to bundle_19 denote the presence of counterfeit notes ranging from one to nineteen notes at positions 1 to 20 within the bundle. Bundle_f represents bundles with all counterfeit notes, while bundle_r signifies genuine bundles with no counterfeit notes. The radar chirp size is set to 8, with a frame size of 40 chirps per frame and an ADC sample rate of 256. This configuration resulted in 81920 data samples per bundle in 2 seconds. After discarding start and end data points, approximately 80,000 data samples remained, we generated 20 RFS per bundle, and each RFS size is set to 5,000 data samples. For each bundle, 400 signals were extracted, resulting in a total of 8,000 RFS per bundle. Considering 21 bundles, the training dataset comprised 168,000 RFS. Additionally, 2400 RFS are reserved separately for testing purposes for each bundle, totaling 50,400 RFS for testing. Therefore, the complete dataset comprised approximately 218,400 samples.

4.3 RFS Preprocessing Feature Extraction

As discussed in the data collection section, we extract the raw data from the mmWave radar, referred to here as RFS. Each RFS possesses three critical identification attributes: the energy magnitude of the signal reflection from detected objects, their radial separation, and the target's velocity. However, the raw RFS captured by each antenna on the mmWave sensor is not suitable for direct use in counterfeit currency detection due to constraints like bandwidth limitations, signal noise, and environmental influences. In indoor environments, RF signals frequently encounter reflections from various static and dynamic objects, such as walls, ceilings, and moving fans. These reflections can mask the essential features of the currency detection process, resulting in a received signal that is a complex amalgamation of multi-path reflections. To mitigate this issue, we employ the Continuous Wavelet Transform (CWT), specifically using the Daubechies wavelet (db1), as illustrated in Fig.4a. After alleviating the multi-path interference from each RFS, we proceed to extract features from each RFS and transform them into a signal scalogram, which is the excellent time-frequency localization properties of this method make it particularly effective for analyzing non-stationary signals, which are common in radar applications.

4.3.1 RFS Preprocessing: One of the essential steps to detect counterfeit currency is to remove various static and dynamic object effects from signals, such as walls, ceilings, moving people, fans, etc. Multi-path interference and background noise are characterized as undesired variations in the RFS, can often interfere with the subsequent analysis, and impede the detection of counterfeit currency. We adopt a noise reduction strategy based on the Daubechies wavelet [55] (particularly the first-order wavelet, or db1).

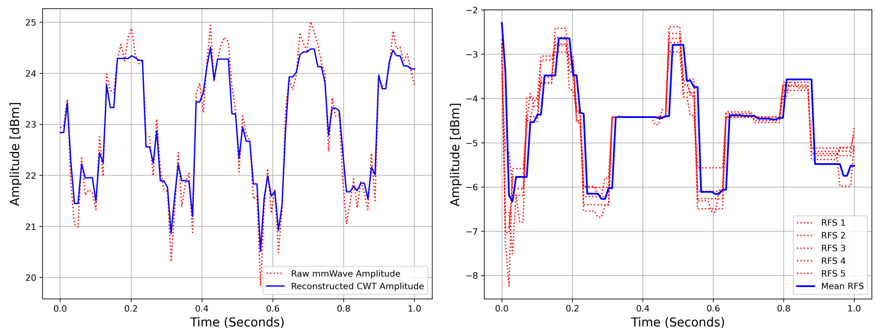

(a) (b)

Fig. 4. Comparative Analysis of Radio Frequency Snapshots (RFS): Fig. 4a Illustrates the Raw and Filtered mmWave RFS. Conversely, Fig. 4b Display the Mean of Five Filtered RFS.

The raw RFS can be mathematically represented as:

$$RFS(t) = s(t) + n(t) \tag{8}$$

where $s(t)$ denotes the clean signal, and $n(t)$ corresponds to the noise. To reduce the noise $n(t)$, we apply a wavelet transform, specifically the db1 wavelet, to $RFS(t)$. The CWT of $RFS(t)$ is given by:

$$w(a, b) = \int RFS(t)\psi^*(a, b)\, dt \tag{9}$$

Here, $\psi^*(a, b)$ represents the complex conjugate of the wavelet, which is dilated by a factor a, and translated by b. $w(a, b)$ describes the local frequency content of $RFS(t)$. This transformation results in the decomposition of the signal into different frequency components. Typically, the high-frequency wavelets encapsulate the noise or transient characteristics in the signal. So, we attenuate these high-frequency wavelets, significantly reducing the RFS's noise content. The denoised RFS, $s(t)$, is then obtained by applying the inverse wavelet transform, given by:

$$s(t) = \frac{1}{|a|^2} \int \int w(a, b)\psi(a, b)\, da\, db \tag{10}$$

This denoised RFS, $s(t)$, is free from extraneous fluctuations as shown in Fig. 4a but retains the vital characteristics of the original signal. Through this mathematical process, we significantly enhance the reliability and clarity of the RFS data, providing a robust foundation for the subsequent stages of our counterfeit currency detection methodology.

4.3.2 RFS Feature Extraction: After converting raw mmWave signals into RFS, we proceed with analyzing the RFS. These RFS initially contain multi-path interferences and background noise, which we systematically removed to enhance clarity and accuracy. The analysis of these cleaned RFS signals, reveals slight pattern variations among signals from the same bundle. These inconsistencies can potentially lower the effectiveness of our system. To maximize our radar

Table 2. Refine RFS Scalograms for Each Currency Bundle

Bundle-1 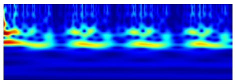	Bundle-2 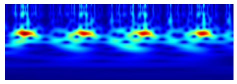	Bundle-3 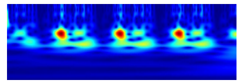	Bundle-4 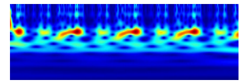	Bundle-5 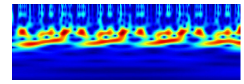
Bundle-6 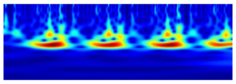	Bundle-7 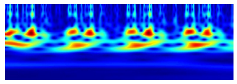	Bundle-8 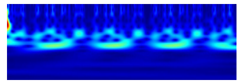	Bundle-9 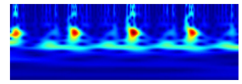	Bundle-10 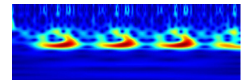
Bundle-11 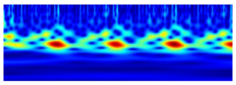	Bundle-12 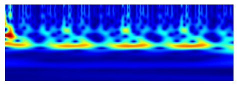	Bundle-13 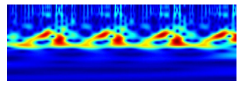	Bundle-14 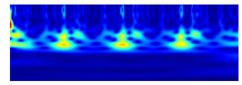	Bundle-15 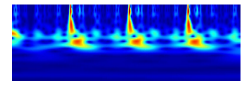
Bundle-16 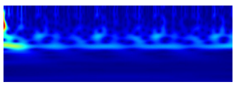	Bundle-17 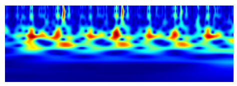	Bundle-18 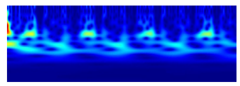	Bundle-19 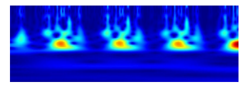	Bundle-20 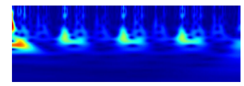

system's reliability and discriminating power, we use a single antenna to handle both the transmission and reception of the RFS. Further refinement involves reducing the complexity of each RFS by limiting the number of data points to 1,000 points. This reduction aids in managing and processing the data more efficiently. For a more robust analysis and to ensure uniformity across our measurements, we make average groups of five RFS, as demonstrated in Fig4b. This approach allows us to represent each bundle with a single, averaged RFS. Initially starting with 8,000 RFS per bundle, this averaging method reduces the total count to 1,600 RFS. This significant reduction decreases the variability within the data and simplifies the feature extraction process, leading to more accurate and discriminative results.

4.3.3 RFS Transformation to Scalograms: In this phase, we transform refined RFS into scalograms, a process crucial for detailed signal analysis. After extensive testing, we have chosen to use the Continuous Wavelet Transform (CWT) [63] with a filter bank approach, specifically referencing the analytical Morlet (amor) wavelet [64]. This choice is informed by the wavelet's superior time-frequency localization properties, which are exceptionally effective for examining non-stationary signals commonly found in radar applications. We configure our system to use a 'voices per octave' setting of 15. This specific setting ensures a balanced trade-off between time and frequency resolution, enabling us to capture critical signal details without high computational costs. The size of each signal for the CWT is defined according to the dimensions of the extracted RFS. The transformed data is visualized using scalograms with a 'jet128' color scheme, and the images are sized at 300x800 pixels. As shown in Table 2, these visualizations play a key role in our analysis, which displays unique scalograms for each note bundle. These bundles vary in the number of counterfeit notes they contain, and the scalograms help in identifying and differentiating these variations effectively.

5 Transferable Learning Model

Just as a human, having learned to identify an object in a picture, can recognize that object in various other pictures taken from different distances, angles, and backgrounds. Our model utilizes signal scalograms to train a transfer learning model for the detection of counterfeit notes within different bundles. In our experiments, we utilize transfer learning for counterfeit currency detection, enabling a system trained on one type of currency to adapt to another with minimal modifications. The model, pre-trained on features of paper material, texture, and patterns from the initial currency, effectively applies these learned features to detect counterfeits in different currencies. This approach significantly reduces the need for extensive data and retraining from scratch. By leveraging knowledge from the original task, our method, mm-CUR, enhances accuracy and accelerates the development process for detecting counterfeit currency across various forms. This model is tasked with learning and predicting the presence of genuine and counterfeit currency via RF sensing. We anticipate that our trained model will successfully detect multiple counterfeit currencies in bundles of varying sizes and tell the exact number of counterfeit notes present in the bundle with its pinpoint location. However, Traditional machine learning algorithms often suffer from substantial performance declines when the test data distribution differs from the training data distribution. To overcome this challenge, we developed a transferable learning model that leverages knowledge from the source domain and seamlessly adapts to new environments using a limited number of samples from the target domain.

Fig. 5 shows that a Heuristic Domain Adaptation [65] based transferable learning model, which operates in four stages. The first stage involves extracting intrinsic features from RFS-based signal scalograms. Next, it identifies the transfer difference between the features of the genuine and counterfeit currency bundles. In the third stage, the transferable difference is removed. Finally, the model uses these features to predict the number of counterfeit notes in bundles with its pinpoint location. This structure ensures that our mm-CUR remains robust and adaptable, maintaining performance across diverse data distributions.

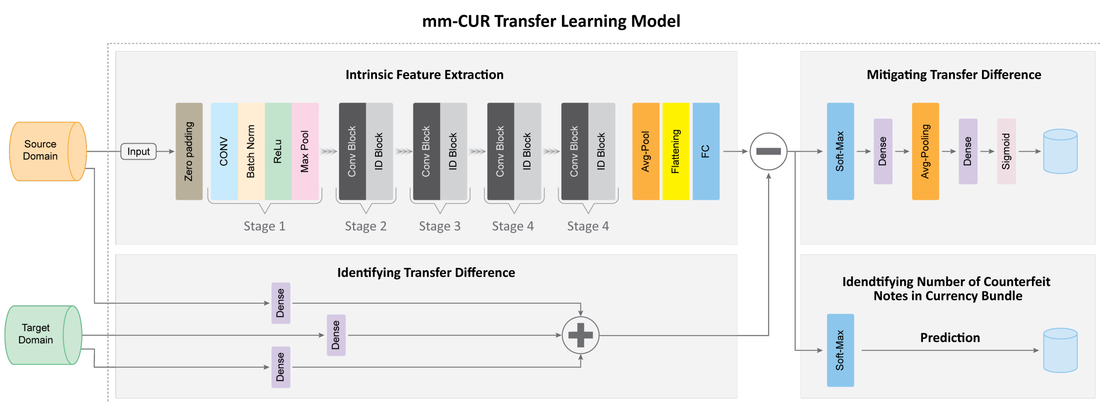

Fig. 5. mm-CUR Transferable Learning Model

5.1 Intrinsic Feature Extraction

Manual extraction of features can be challenging and there's a risk of omitting information pertinent to currency identification. We used neural networks to circumvent these difficulties and extract reliable feature representations. Specifically, we employ ResNet-50 [66] to derive the features $S(x_i)$ where x_i represents the RFS scalograms. The Pre-trained model called ResNet-50 is chosen for intrinsic information extraction due to its proficiency in combining low-level local information with high-level global information from deeper network layers. Its unique design, featuring residual connections, adds to the network's flexibility, making it a powerful tool for our feature extraction process.

5.2 Mitigating of Transfer Difference

We use a Generative Adversarial Network (GAN)[67] to handle transfer differences, specifically harnessing its architecture to extract intrinsic information. The GAN model comprises two primary components: the generator and the discriminator. The role of the generator is to extract the features $F(x_i)$, where x_i denotes the RFS scalograms. Conversely, the discriminator's role is to determine if the signal representation originates from the source or target domain. To enhance the process, we incorporate a gradient reversal layer into the discriminator, facilitating simultaneous training of both the discriminator and generator.

The signal scalograms, which can be from either the source or target domain, serve as an input to the generator, producing an output feature representation. Subsequently, this feature representation is input into the discriminator, which discerns between the source and target domains. The generator's loss function is defined as $L_G = -E_{x_i^n \sim D_N} \log D(F_i)$, where F_i and x_i denote the feature and signal scalograms in the source domain, respectively; D represents the identifier; and D_N signifies the source domain sample set. Similarly, the discriminator's loss function is formulated as

Algorithm 1 mm-CUR Algorithm

Input: RFS: RF signal
Output: N_c: Number of counterfeit notes
procedure mm-CUR(RFS)
  for each s_i in RFS **do**
    Process s_i and refine it
    $s_i' \leftarrow \textsc{Refine}(s_i)$
    $s_i'' \leftarrow \textsc{NoiseFilter}(s_i')$
    $s_i''' \leftarrow \text{HPF}(s_i'')$
  end for
  $\bar{s} \leftarrow \textsc{Mean}(s_i''', 5)$
  for each rfs_i in $\bar{s}$ **do**
    Scale rfs_i
    $S_i \leftarrow \textsc{Scal}(rfs_i)$
  end for
  $M \leftarrow \textsc{Train}(S)$
  $N_c \leftarrow \textsc{Detect}(M)$
end procedure

$L_D = -E_{x_i^n \sim D_N} \log D(F_i) + E_{x_j^a \sim D_A}[-\log(1 - D(F_j))]$ with F_j and x_j representing the feature and target domain representation, respectively; and D_A signifying the sample set from the target domain. Upon completion of training, the generator becomes adept at generating feature representations that encapsulate the fundamental attributes of currency detection, adaptable to varying environmental conditions.

5.3 Identifying Genuine and Counterfeit Currency

After the removal of transfer differences from the feature representations, we employ a deep neural network (DNN) to distinguish between genuine and counterfeit currency within a bundle, eliminating the need to inspect each note. The loss for the DNN is articulated as $L_p = L_{CE}(F(x_i) - H(x_i), y_i)$, where y_i represents the label for the sample (either genuine or counterfeit), and L_{CE} stands for the cross-entropy between the variables.

5.4 Implementation

As shown in Fig. 5, We employ ResNet-50 for the source domain and integrate the intrinsic information extraction module. In the target domain, we configure three dense layers with 512 neurons, employing max pooling and a ReLU function to generate domain information and recognize transfer information between the source and target domains. To address transfer differences, we introduce a GAN model with two dense layers having 512 neurons each, utilizing max pooling and a sigmoid function to produce domain information. Finally, a SoftMax layer provides the ultimate prediction, distinguishing between genuine and counterfeit notes while pinpointing their location in the bundle.

Table 3. List of Parameter used in mm-CUR Experiment

Parameters/Symbols	Value
Start Frequency f_{Start}	77 GHz
Number of Channels, N	1
Chirp Duration T_C	$40\mu s$
Chirp Bandwidth, B	4 GHz
IF Bandwidth, IF_{Max}	15 MHz
Ramp Chirp Rate, S	$100 MHz\mu s$
ADC Sampling Rate	256 MHz
Detection Range R_d	0.3 m
Chirp Size	8
Frame Size	40
Voice Per Octaves	15
RFS Length	1000 data points
CWT Wavelet Type	Analytical Morlet (Amor)
Scalogram Color	Jet128

6 Results and Discussion

We undertake comprehensive experiments to assess mm-CUR performance, aiming to address the following questions:

- **Q1:** Can mm-CUR reliably detect counterfeit currency within note bundles with a high degree of accuracy?
- **Q2:** How instrumental is mm-CUR design in influencing prediction accuracy?
- **Q3:** Does mm-CUR maintain its robustness across varied scenarios?

6.1 Experimental Setup

We utilize and adjust the TI-IWR1443 integrated mmWave FMCW radar sensor module from TI [55] to operate within the 77–81 GHz frequency range. As depicted in Fig. 3a, The radar is positioned in a tabletop setup, 20 cm above the currency bundle, to collect data effectively. We implemented the algorithms using Python 3.7 on Jupiter Notebook, executed on a MacBook equipped with a 2.4GHz Intel Core i5 CPU and 8GB RAM, running the Mac operating system. This MacBook is linked to the DCA1000EVM via an Ethernet cable. We obtained 21 bundles of authentic 100-yuan notes from a local Chinese bank, and integrated counterfeit notes into various locations within each bundle, introducing from 1 up to 20 counterfeit notes. we used acidic, printed, and locally made counterfeit currency notes, the main properties used for detection are paper material, watermarks, and holographic elements, which exhibit specific patterns in genuine currency. The data samples are labeled as 'bundle_1' contains 1 counterfeit note at different locations (1-20), 'bundle_2' contains 2, and so on up to bundle 19. 'bundle_f' indicates a fully counterfeit note bundle, while 'bundle_r' represents all genuine note bundles. For our experimental setup, we used single transmission (TX) and receiving (RX) channels to

Table 4. mm-CUR Classification Report

Classes	Precision	Recall	F1-Score
Bundle-1	0.64	1.0	0.78
Bundle-2	1.0	1.0	1.0
Bundle-3	1.0	1.0	1.0
Bundle-4	1.0	1.0	1.0
Bundle-5	0.9	1.0	0.94
Bundle-6	1.0	0.88	0.94
Bundle-7	1.0	1.0	1.0
Bundle-8	1.0	1.0	1.0
Bundle-9	1.0	1.0	1.0
Bundle-10	1.0	1.0	1.0
Bundle-11	1.0	1.0	1.0
Bundle-12	0.83	1.0	0.88
Bundle-13	1.0	0.81	0.9
Bundle-14	0.81	1.0	0.88
Bundle-15	1.0	0.81	0.9
Bundle-16	1.0	1.0	1.0
Bundle-17	1.0	1.0	1.0
Bundle-18	1.0	0.88	0.94
Bundle-19	0.90	1.0	0.95
Bundle-f	1.0	0.75	0.85
Bundle-r	1.0	0.83	0.90
Overall Accuracy	-	-	0.93

gather the dataset. f_{Start} is the initial frequency of FMCW radar chipsets and is fixed at 77 GHz, with a sweep bandwidth is B, of 4 GHz. The IF bandwidth of the chipset supports 15 MHz. The radar chirp's duration T_C, is set to $40\mu s$. So, determining the ramp chirp rate $S = B/T_C$ = 100MHz. $Range_{\text{Max}} = (IF_{\text{Max}} \times C)/(2 \times S)$, is the maximum detectable range, where IF_{Max}, C, and S are the maximum IF bandwidth, speed of light, and chirp ramp rate. The radar ADC sampling rate is set to 256 MHz, each frame size contains 8 chirps with a detecting range of 20cm. The raw data from the RX channel produces 1 × 81920 data samples, which are then preprocessed into RFS as input for various identification methodologies. A comprehensive breakdown of the radar module's parameters used to collect the data can be found in Table 3. The experimental setup is consistently applied to each currency bundle. Although the signal introduced by the background may influence the measurements, its impact is negligible and overlooked by the classifier. Data collection spanned multiple sessions over a week, ensuring diversity in the collection environments. For every currency bundle type, we divided the physical samples into two segments: one for training data collection and the other for testing. Importantly, the testing data hasn't been seen by the transfer learning classifier.

6.2 Experimental Results

We assessed the efficiency of mm-CUR on the 21 currency bundles, with the outcomes detailed in Table 4. Notably, mm-CUR boasts an average accuracy of 93% in distinguishing between genuine and counterfeit notes and detects the

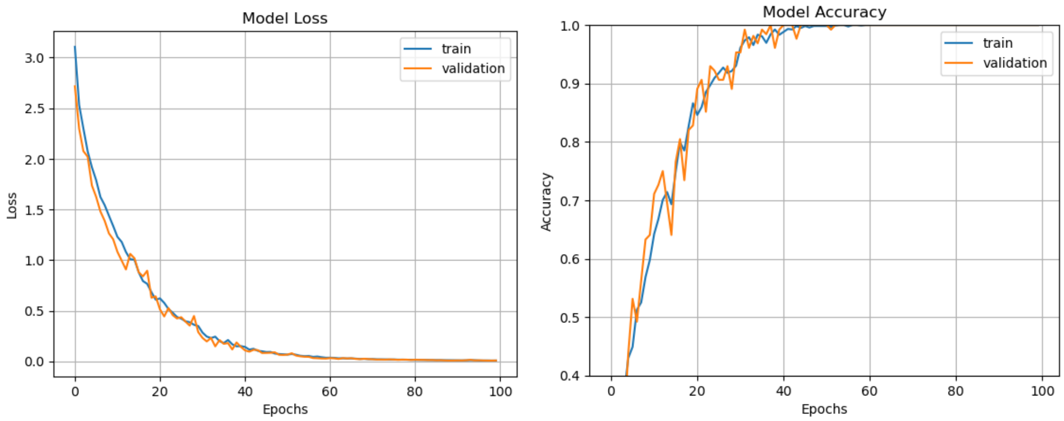

(a) (b)

Fig. 6. (a) and (b), Illustrate the Model Accuracy and Loss During Training.

pinpoint location and the number of counterfeit notes in each bundle without checking individual notes. Most of the currency bundles achieved 100% perfect scores in precision, recall, and F1-Score as shown in Fig. 11. Moreover, across all bundles, both the false alarm rate and the missing alarm rate remain impressively low, and the accuracy of mm-CUR to various currency types using the transferable learning model is relatively high. In Fig. 7 the confusion matrix reveals that some bundles show a false alarm rate. A potential reason is that the scalograms of these bundles exhibit identical features in certain areas. We aim to delve deeper into this in our subsequent research, to eliminate any ambiguities.

6.3 Location-aware Evaluation of mm-CUR

We evaluated the mm-CUR location-aware counterfeit currency detection using a bundle of 100 notes in different scenarios: Scenario 1, Scenario 2, and Scenario 3. In each scenario, we placed 1, 2, and 3 counterfeit notes within the bundle at 5 different locations (4th, 8th, 12th, 16th, and 20th locations). Specifically, we aimed to detect counterfeit currency notes placed at various locations within the bundle. To assess the impact of location changes, we collected data from 5 bundles, each containing one, two, or three counterfeit notes, from a mmWave distance of 20 cm, the mmWave sensor was connected to a laptop, and positioned on a tabletop. We collected 20 RFS based on their location in the bundle. After evaluation, we achieved a high accuracy rate of 91.3 % in detecting counterfeit notes at different locations. Fig.8a, 8b, and 8c show the confusion matrices, proving that mm-CUR can effectively detect counterfeit currency notes at various locations within the bundle.

6.4 Distance-Based Evaluation of mm-CUR

In the context of detecting counterfeit currency within bundles using the mmWave sensor, the distance between the sensor antennas and the target currency bundle is crucial. We conducted extensive experiments at varying distances from 1 to 45 cm, as shown in Fig. 9a. Our findings revealed that at a distance of 20 cm, both the average amplitude and phase of the mmWave signals change gradually rather than abruptly. This distance also produced higher accuracy rates as shown in Fig.9b, compared to other distances. This optimal distance allowed for more reliable and precise measurements, enhancing the overall effectiveness of the detection process. Based on consistent results across various

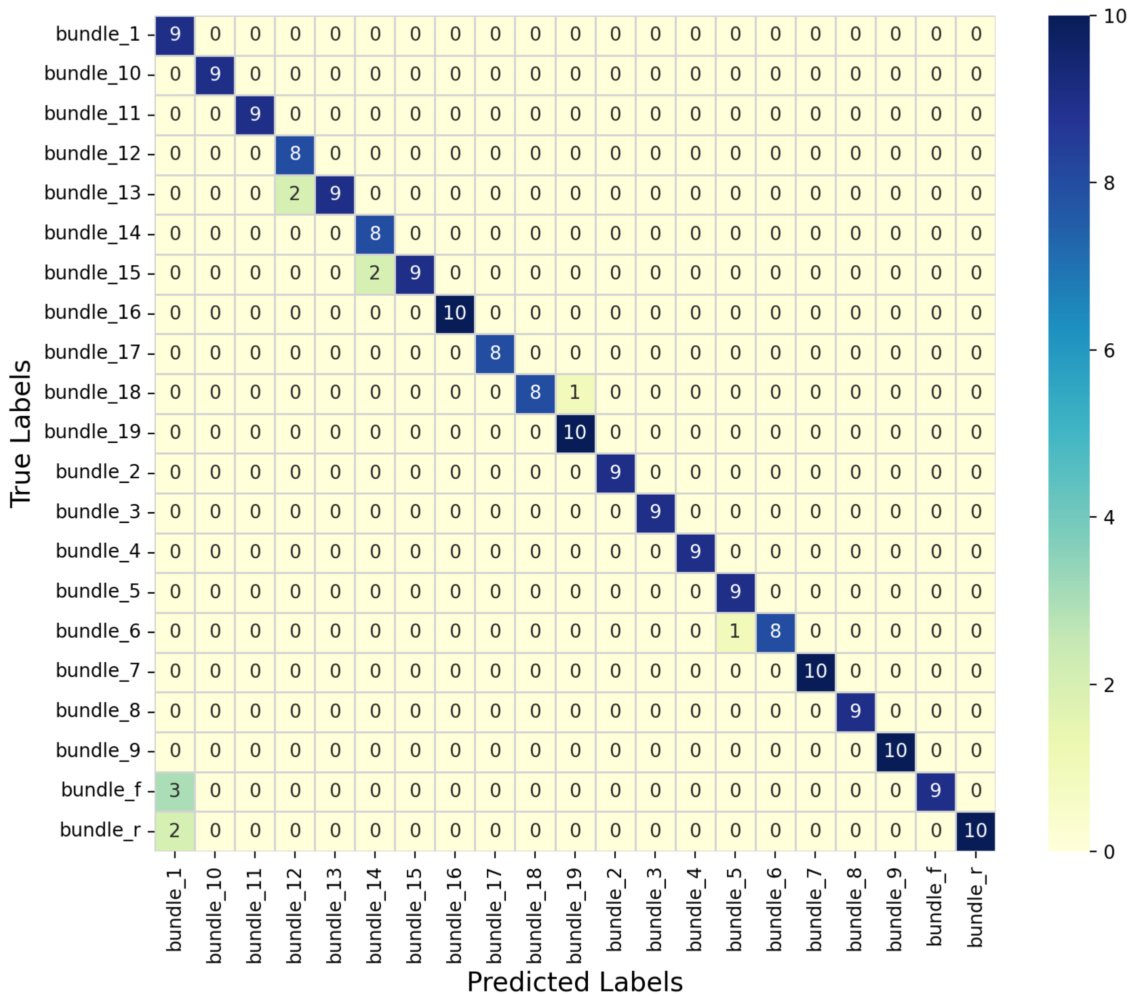

Fig. 7. mm-CUR Confusion Matrix

types of currency bundles, we have determined that positioning the radar at a distance of 20 cm is optimal for detecting counterfeit notes. This distance minimizes sharp signal fluctuations and maximizes detection accuracy, making it the most effective setup for our system.

6.5 Ablation Study

We evaluated the effectiveness of mm-CUR in terms of RFS refinement, scalogram features extraction, mmWave Sensor Deployment at different Distances, and transferable learning model.

RFS Refinement: The performance of mm-CUR was tested by changing the number of chirps used for the Radio Frequency Snapshots (RFS). A chirp refers to a type of signal or pulse. The tests were conducted with different counts of these chirps: 4, 8, 12, 16, and 20. As shown in Fig. 10, when using only 4 chirps, the detection accuracy of mm-CUR was

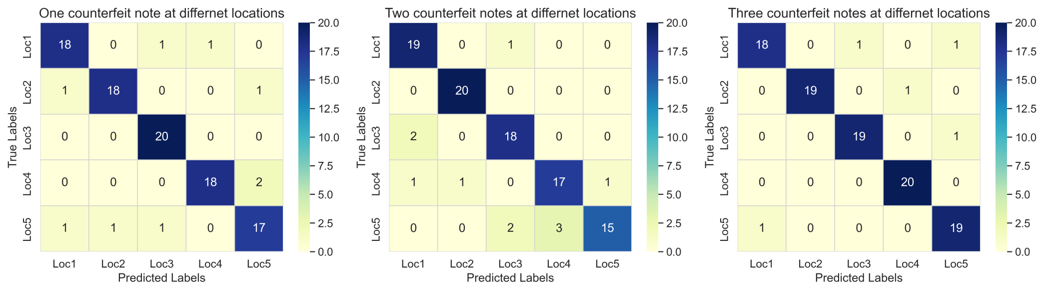

(a) (b) (c)

Fig. 8. Location-aware Evaluation of mm-CUR. Fig. 8a, 8b, and 8c Show Effective Detection of Counterfeit Currency Notes at Various Locations within the Bundle.

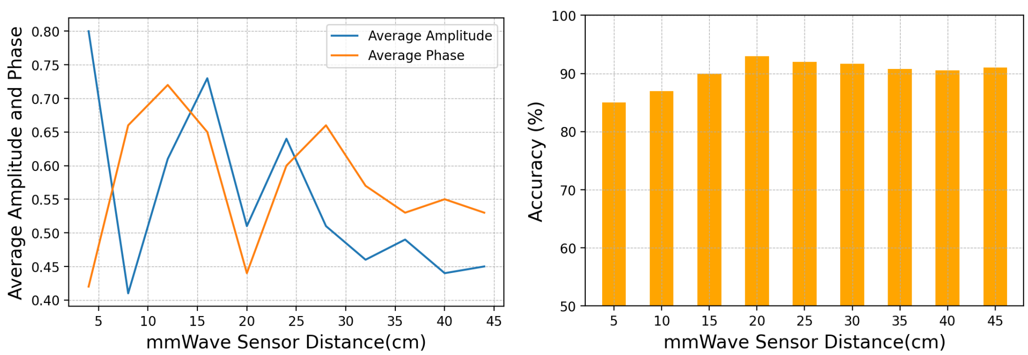

(a) (b)

Fig. 9. Distance-based Evaluation of mm-CUR: Fig. 4a Illustrates the Average Amplitude and Phase of Raw mmWave Signals. Conversely, Fig. 4b the Accuracy of mm-CUR at Different Distances.

92%. Increasing the number of chirps to 8 improved the accuracy slightly to 93%. This is the highest accuracy achieved. However, if we continue to increase the number of chirps beyond 8 (to 12, 16, and 20), the accuracy starts to drop. For instance, the accuracy dropped to 88%, 85.5%, and 83.1% respectively. A possible reason for this trend could be the surge in out-of-order packets with an increase in chirps rate.

Transferable Learning Model: We conducted a comparative performance analysis between our proposed transferable learning model and conventional models i-e. the Convolutional Neural Network (CNN) and Deep Neural Network (DNN). For each currency bundle, we trained a ResNet-50 network utilizing all available data samples. The performance of these trained models, when tested across different bundles achieved better results. Fig. 6a, 6b, and 10a, 10b indicate that the transferable learning model detects counterfeit notes in buddle with high accuracy and stability as compared to traditional models.

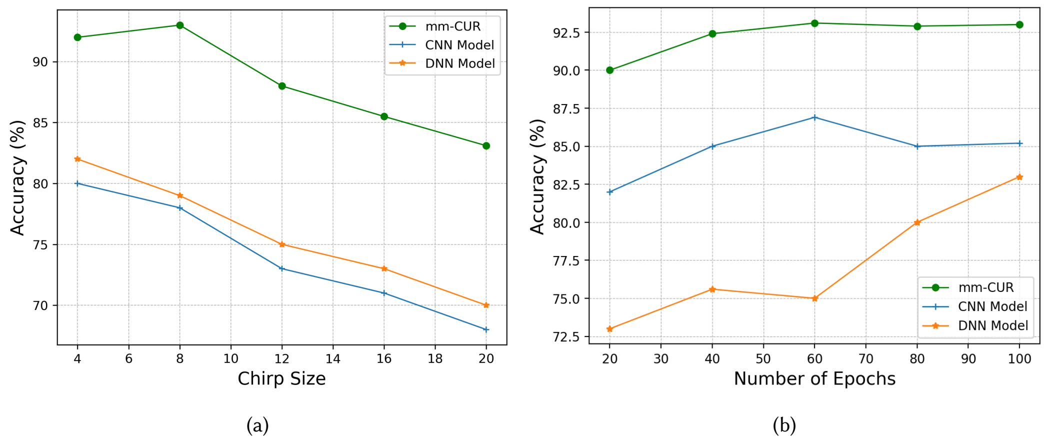

Fig. 10. (a) and (b), Illustrate the Comparison of the mm-CUR Model with Traditional Models.

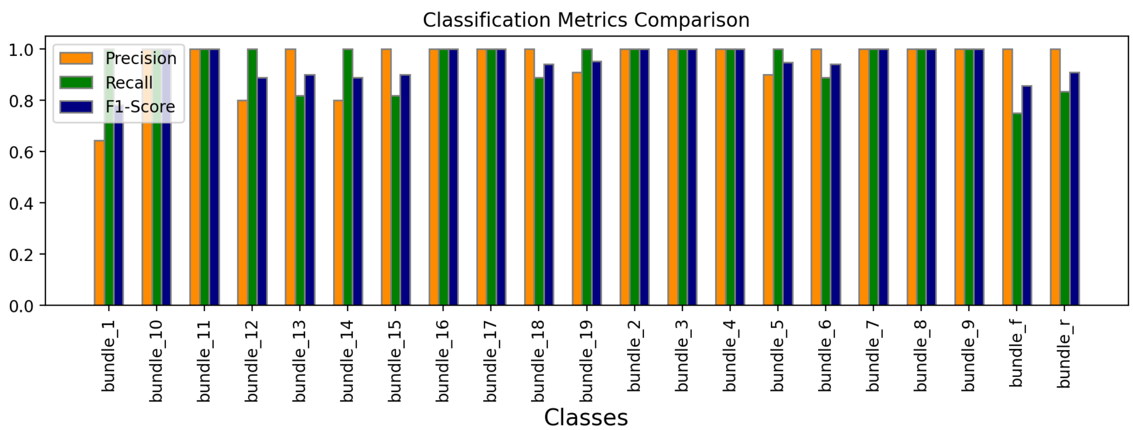

Fig. 11. Precision, Recall, and F1-Score for each Counterfeit Currency Bundle

6.6 Robustness

Impact of Distances: We demonstrate mm-CUR robustness across varying distances between the table end and the radar device specifically at distances of 4cm to 45cm. At each of these intervals, we collected data samples from all currency bundles. As illustrated in Fig. 12a, 12b, mm-CUR consistently delivers high accuracy regardless of the distance. The recorded average accuracy is 88%, 90.1%, 93%, 92.2%, and 91%. Notably, detection accuracy decreases as the distance increases. This is attributed to the RF signal attenuation that occurs as the gap between the bundle's end and the radar device increases. A unique observation is a dip in average accuracy at the 45cm mark, this is because the transferable learning model training data predominantly feature scenes with distances shorter than 20cm.

Impact of Training Set Size: Since we used the transferable learning model, the size of the training dataset plays an important role in influencing system performance and reliability. Fig. 12b elucidates the correlation between the size of the training dataset and the detection accuracy of the model. Increasing the training size to 80% improved accuracy

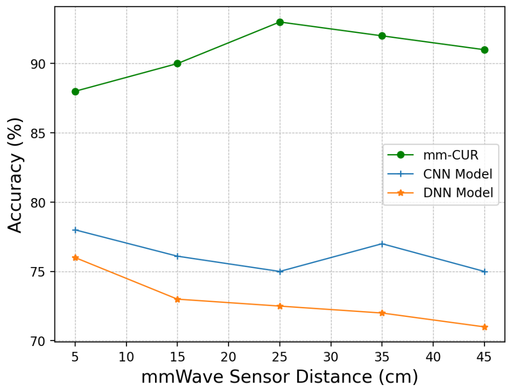

(a)

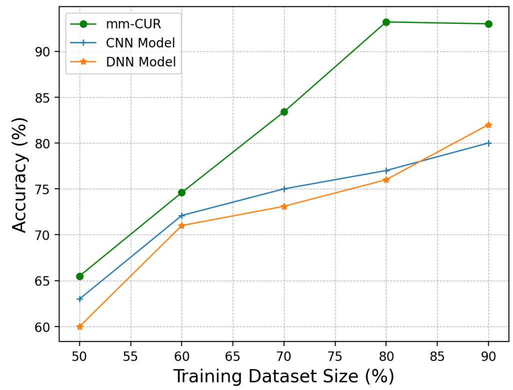

(b)

Fig. 12. (a) and (b) Illustrate the mm-CUR Model Robustness Comparison with Deep Learning Models in Terms of Distance and Training Size

slightly to 93%. This is the highest accuracy achieved. Notably, as the training dataset increases, mm-CUR accuracy witnesses a sharp ascent as compared to the traditional deep learning models.

7 Future work and Limitation

We have developed an initial prototype of mm-CUR that successfully performs data acquisition, signal preprocessing, scalogram feature extraction, and counterfeit currency identification under optimal conditions. However, to evolve mm-CUR into a commercially viable solution applicable to various currencies, several practical challenges need to be addressed.

7.1 Currency-Independent Framework

Our research indicates that mm-CUR can be calibrated for currency detection using a minimal subset of samples from each bundle of Chinese yuan notes. Yet, when introduced to unfamiliar data sets of bundle notes, the pre-trained model, based on prior bundles, yields an accuracy below 60%. Attaining complete currency independence for mm-CUR is both desirable and challenging. We envision three possible potential future directions to address this limitation.

- **Hardware Specifications:** Utilizing more advanced radar devices capable of capturing intricate signals would significantly enhance the detection efficacy of mm-CUR. This enhancement extends to its applicability to other currencies as well.
- **Learning Enhanced Representations:** To improve counterfeit currency detection precision, a promising strategy is to refine the extraction of representations within bundle notes from radar signals. Currently, idiosyncratic variations have a notable impact on mm-CUR detection accuracy. By integrating state-of-the-art representation learning methods, we aim to isolate currency-independent features that are specifically relevant to counterfeit detection.

- **Employing Meta-learning:** Meta-learning is emerging as a promising strategy to transfer knowledge from one domain to another. Future efforts could utilize meta-learning to enhance the versatility of mm-CUR. For instance, integrating data from analogous tasks could serve as a means to bolster the detection efficacy of mm-CUR.

7.2 Addressing Complex Situations

Our evaluations of mm-CUR have focused on standard parameters, such as fixed distances, dataset sizes, chirp frequencies, and the number of epochs. However, more complex scenarios could present challenges to the system's performance. Exploring these nuanced situations is crucial to fully understanding and enhancing the robustness and reliability of mm-CUR in diverse and unpredictable environments.

- **Environmental Factors:** The surrounding environment can greatly affect the performance of mm-CUR. Factors such as ambient temperature, humidity, and the type of materials present nearby can influence RF signal propagation. It is important to investigate the system's efficacy in diverse settings, ranging from controlled indoor laboratories to bustling outdoor locations. Understanding how mm-CUR performs across various environments will aid in refining its algorithms and enhancing its robustness.
- **Number of People around the Table:** Human bodies can absorb, reflect, and refract RF signals, depending on their positioning and movement. As the number of individuals around the table increases, the potential for interference or signal distortion also rises. Evaluating mm-CUR performance with varying numbers of people, from a solitary individual to a crowded setting, is essential. This assessment will help determine the system's resilience against human-induced perturbations and its ability to maintain counterfeit detection accuracy regardless of crowd density.
- **Old and New Currency Notes:** The physical condition of currency notes can significantly impact the reflection and absorption of RF signals. Old, worn-out notes may have creases, smudges, or small tears that can alter the signal differently compared to the crisp, new currency. It is crucial to evaluate how effectively mm-CUR can distinguish between genuine and counterfeit notes across both old and new currency materials. This evaluation ensures the system's reliability throughout the entire lifespan of a banknote.
- **Presence of Other RF Devices Near the Radar:** In today's world, RF devices are ubiquitous, including smartphones, WiFi routers, and other specialized equipment. The operation of these devices near the radar can lead to potential issues such as signal interference, crosstalk, and harmonic distortions. Evaluating the performance of mm-CUR in environments with other RF devices is essential to determine its effectiveness in everyday settings where multiple RF devices are common. This assessment will also help identify if any shielding or adaptive algorithms are necessary to mitigate interference and ensure reliable operation.

8 Conclusion

In this paper, we introduced mm-CUR, an innovative system that utilizes a commercial 77-81 GHz networking chipset to detect location-aware counterfeit currency within note bundles by reusing mmWave radar RF. Utilizing RF signal scalograms, mm-CUR offers a contact-free, universally applicable, and intuitive method for detecting counterfeit currency by leveraging intrinsic features through transfer learning. advanced algorithms to extract valuable signal information from Radio Frequency Snapshots (RFS) and enhanced signal clarity by filtering out noise using Continuous Wavelet Transform (CWT). A transfer learning model is then applied to the scalograms of currency bundles, enabling precise identification of counterfeit notes. We conducted extensive evaluations on mm-CUR using 21 distinct note bundles. The results affirm the system's proficiency in detecting counterfeit currency under real-world conditions. Beyond its immediate application, mm-CUR illustrates the potential of re-purposing mmWave networking devices in the currency domain, opening avenues for future explorations.

References

[1] Ji Woo Lee, Hyung Gil Hong, Ki Wan Kim, and Kang Ryoung Park. A survey on banknote recognition methods by various sensors. *Sensors*, 17:313, 2017.

[2] Shuai Wang, Luoyu Mei, Zhimeng Yin, Hao Li, Ruofeng Liu, Wenchao Jiang, and Chris Xiaoxuan Lu. End-to-end target liveness detection via mmwave radar and vision fusion for autonomous vehicles. *ACM Transactions on Sensor Networks*, 2023.

[3] Fei Shang, Panlong Yang, Jie Xiong, Yuanhao Feng, and Xiangyang Li. Tamera: Contactless commodity tracking, material and shopping behavior recognition using cots rfids. *ACM Transactions on Sensor Networks*, 19(2):1–24, 2023.

[4] Andrei A Bunaciu, Elena Gabriela UdriŞTioiu, and Hassan Y Aboul-Enein. X-ray diffraction: instrumentation and applications. *Critical reviews in analytical chemistry*, 45:289–299, 2015.

[5] Temitope D Timothy Oyedotun. X-ray fluorescence (xrf) in the investigation of the composition of earth materials: a review and an overview. *Geology, Ecology, and Landscapes*, 2(2):148–154, 2018.

[6] C Fiorini and A Longoni. In-situ, non-destructive identification of chemical elements by means of portable edxrf spectrometer. *IEEE Transactions on nuclear science*, 46(6):2011–2016, 1999.

[7] Gerd Dobmann, Iris Altpeter, Christoph Sklarczyk, and Roman Pinchuk. Non-destructive testing with micro-and mm-waves—where we are—where we go. *Welding in the World*, 56(1-2):111–120, 2012.

[8] Akram Al-Hourani, Robin J Evans, Peter M Farrell, Bill Moran, Marco Martorella, Sithamparanathan Kandeepan, Stan Skafidas, and Udaya Parampalli. Millimeter-wave integrated radar systems and techniques. In *Academic Press Library in Signal Processing, Volume 7*, pages 317–363. Elsevier, 2018.

[9] Yi Zhang, Zheng Yang, Guidong Zhang, Chenshu Wu, and Li Zhang. Xgest: Enabling cross-label gesture recognition with rf signals. *ACM Transactions on Sensor Networks (TOSN)*, 17(4):1–23, 2021.

[10] Sruthy Skaria, Akram Al-Hourani, Margaret Lech, and Robin J Evans. Hand-gesture recognition using two-antenna doppler radar with deep convolutional neural networks. *IEEE Sensors Journal*, 19(8):3041–3048, 2019.

[11] Chris Xiaoxuan Lu, Stefano Rosa, Peijun Zhao, Bing Wang, Changhao Chen, John A Stankovic, Niki Trigoni, and Andrew Markham. See through smoke: robust indoor mapping with low-cost mmwave radar. In *Proceedings of the 18th International Conference on Mobile Systems, Applications, and Services*, pages 14–27, 2020.

[12] Xin Yang, Jian Liu, Yingying Chen, Xiaonan Guo, and Yucheng Xie. Mu-id: Multi-user identification through gaits using millimeter wave radios. In *IEEE INFOCOM 2020-IEEE Conference on Computer Communications*, pages 2589–2598. IEEE, 2020.

[13] Guidong Zhang, Guoxuan Chi, Yi Zhang, Xuan Ding, and Zheng Yang. Push the limit of millimeter-wave radar localization. *ACM Transactions on Sensor Networks*, 19(3):1–21, 2023.

[14] Tianyue Zheng, Zhe Chen, Chao Cai, Jun Luo, and Xu Zhang. V2ifi: In-vehicle vital sign monitoring via compact rf sensing. *Proceedings of the ACM on Interactive, Mobile, Wearable and Ubiquitous Technologies*, 4(2):1–27, 2020.

[15] Zhicheng Yang, Parth H Pathak, Yunze Zeng, Xixi Liran, and Prasant Mohapatra. Vital sign and sleep monitoring using millimeter wave. *ACM Transactions on Sensor Networks (TOSN)*, 13(2):1–32, 2017.

[16] Akarsh Prabhakara, Vaibhav Singh, Swarun Kumar, and Anthony Rowe. Osprey: A mmwave approach to tire wear sensing. In *Proceedings of the 18th international conference on mobile systems, applications, and services*, pages 28–41, 2020.

[17] Mingmin Zhao, Kreshnik Hoti, Hao Wang, Aniruddh Raghu, and Dina Katabi. Assessment of medication self-administration using artificial intelligence. *Nature medicine*, 27(4):727–735, 2021.

[18] Baicheng Chen, Huining Li, Zhengxiong Li, Xingyu Chen, Chenhan Xu, and Wenyao Xu. Thermowave: a new paradigm of wireless passive temperature monitoring via mmwave sensing. In *Proceedings of the 26th Annual International Conference on Mobile Computing and Networking*, pages 1–14, 2020.

[19] Chen Wang, Jian Liu, Yingying Chen, Hongbo Liu, and Yan Wang. Towards in-baggage suspicious object detection using commodity wifi. In *2018 IEEE Conference on Communications and Network Security (CNS)*, pages 1–9. IEEE, 2018.

[20] Seung-Hoon Chae, Jong Kwang Kim, and Sung Bum Pan. A study on the korean banknote recognition using rgb and uv information. In *International Conference on Future Generation Communication and Networking*, pages 477–484. Springer, 2009.

[21] K Kang and C Lee. Fake banknote detection using multispectral images. In *2016 7th International Conference on Information, Intelligence, Systems & Applications (IISA)*, pages 1–3. IEEE, 2016.

[22] Sangwook Baek, Euisun Choi, Yoonkil Baek, and Chulhee Lee. Detection of counterfeit banknotes using multispectral images. *Digital Signal Processing*, 78:294–304, 2018.

[23] Miseon Han and Jeongtae Kim. Joint banknote recognition and counterfeit detection using explainable artificial intelligence. *Sensors*, 19(16):3607, 2019.

[24] Arcangelo Bruna, Giovanni Maria Farinella, Giuseppe Claudio Guarnera, and Sebastiano Battiato. Forgery detection and value identification of euro banknotes. *Sensors*, 13(2):2515–2529, 2013.

[25] R Bhavani and A Karthikeyan. A novel method for counterfeit banknote detection. *Int. J. Comput. Sci. Eng*, 2(4):165–167, 2014.

[26] Chi-Yuan Yeh, Wen-Pin Su, and Shie-Jue Lee. Employing multiple-kernel support vector machines for counterfeit banknote recognition. *Applied Soft Computing*, 11(1):1439–1447, 2011.

[27] Keon-Ho Lee and Tae-Hyoung Park. Image segmentation of uv pattern for automatic paper-money inspection. In *2010 11th International Conference on Control Automation Robotics & Vision*, pages 1175–1180. IEEE, 2010.

[28] Ankush Roy, Biswajit Halder, Utpal Garain, and David S Doermann. Machine-assisted authentication of paper currency: an experiment on indian banknotes. *International Journal on Document Analysis and Recognition (IJDAR)*, 18(3):271–285, 2015.

[29] Minemasa Hida, Toshiyuki Mitsui, and Yukio Minami. Forensic investigation of counterfeit coins. *Forensic science international*, 89(1-2):21–26, 1997.

[30] Fan Liu, Longfei Zhou, Christos Masouros, Ang Li, Wu Luo, and Athina Petropulu. Toward dual-functional radar-communication systems: Optimal waveform design. *IEEE Transactions on Signal Processing*, 66(16):4264–4279, 2018.

[31] Le Zheng, Marco Lops, Yonina C Eldar, and Xiaodong Wang. Radar and communication coexistence: An overview: A review of recent methods. *IEEE Signal Processing Magazine*, 36(5):85–99, 2019.

[32] Aboulnasr Hassanien, Moeness G Amin, Elias Aboutanios, and Braham Himed. Dual-function radar communication systems: A solution to the spectrum congestion problem. *IEEE Signal Processing Magazine*, 36(5):115–126, 2019.

[33] Zhengxiong Li, Zhuolin Yang, Chen Song, Changzhi Li, Zhengyu Peng, and Wenyao Xu. E-eye: Hidden electronics recognition through mmwave nonlinear effects. In *Proceedings of the 16th ACM Conference on Embedded Networked Sensor Systems*, pages 68–81, 2018.

[34] Chenshu Wu, Zheng Yang, Zimu Zhou, Xuefeng Liu, Yunhao Liu, and Jiannong Cao. Non-invasive detection of moving and stationary human with wifi. *IEEE Journal on Selected Areas in Communications*, 33(11):2329–2342, 2015.

[35] Ashutosh Dhekne, Mahanth Gowda, Yixuan Zhao, Haitham Hassanieh, and Romit Roy Choudhury. Liquid: A wireless liquid identifier. In *Proceedings of the 16th annual international conference on mobile systems, applications, and services*, pages 442–454, 2018.

[36] Ju Wang, Jie Xiong, Xiaojiang Chen, Hongbo Jiang, Rajesh Krishna Balan, and Dingyi Fang. Tagscan: Simultaneous target imaging and material identification with commodity rfid devices. In *Proceedings of the 23rd Annual International Conference on Mobile Computing and Networking*, pages 288–300, 2017.

[37] Shichao Yue and Dina Katabi. Liquid testing with your smartphone. In *Proceedings of the 17th Annual International Conference on Mobile Systems, Applications, and Services*, pages 275–286, 2019.

[38] Hui-Shyong Yeo, Gergely Flamich, Patrick Schrempf, David Harris-Birtill, and Aaron Quigley. Radarcat: Radar categorization for input & interaction. In *Proceedings of the 29th Annual Symposium on User Interface Software and Technology*, pages 833–841, 2016.

[39] Yumeng Liang, Anfu Zhou, Huanhuan Zhang, Xinzhe Wen, and Huadong Ma. Fg-liquid: A contact-less fine-grained liquid identifier by pushing the limits of millimeter-wave sensing. *Proceedings of the ACM on Interactive, Mobile, Wearable and Ubiquitous Technologies*, 5(3):1–27, 2021.

[40] Xiaoying Yang and Yang Zhang. Cubesense: Wireless, battery-free interactivity through low-cost corner reflector mechanisms. In *Extended Abstracts of the 2021 CHI Conference on Human Factors in Computing Systems*, pages 1–6, 2021.

[41] Hui-Shyong Yeo, Ryosuke Minami, Kirill Rodriguez, George Shaker, and Aaron Quigley. Exploring tangible interactions with radar sensing. *Proceedings of the ACM on Interactive, Mobile, Wearable and Ubiquitous Technologies*, 2(4):1–25, 2018.

[42] Zhengxiong Li, Baicheng Chen, Zhuolin Yang, Huining Li, Chenhan Xu, Xingyu Chen, Kun Wang, and Wenyao Xu. Ferrotag: A paper-based mmwave-scannable tagging infrastructure. In *Proceedings of the 17th Conference on Embedded Networked Sensor Systems*, pages 324–337, 2019.

[43] Riku Arakawa and Yang Zhang. Low-cost millimeter-wave interactive sensing through origami reflectors. In *CHIIoT@ EWSN/EICS*, 2021.

[44] Diana Zhang, Jingxian Wang, Junsu Jang, Junbo Zhang, and Swarun Kumar. On the feasibility of wi-fi based material sensing. In *The 25th Annual International Conference on Mobile Computing and Networking*, pages 1–16, 2019.

[45] Meng Xue, Yanjiao Chen, Xueluan Gong, Jian Zhang, and Chunkai Fan. Wet-ra: Monitoring diapers wetness with wireless signals. *Proceedings of the ACM on Interactive, Mobile, Wearable and Ubiquitous Technologies*, 6(2):1–26, 2022.

[46] Fahim Niaz, Muhammad Khalid, Zahid Ullah, Nauman Aslam, Mohsin Raza, and MK Priyan. A bonded channel in cognitive wireless body area network based on ieee 802.15. 6 and internet of things. *Computer Communications*, 150:131–143, 2020.

[47] Huining Li, Chenhan Xu, Aditya Singh Rathore, Zhengxiong Li, Hanbin Zhang, Chen Song, Kun Wang, Lu Su, Feng Lin, Kui Ren, et al. Vocalprint: exploring a resilient and secure voice authentication via mmwave biometric interrogation. In *Proceedings of the 18th Conference on Embedded Networked Sensor Systems*, pages 312–325, 2020.

[48] Kun Qian, Chenshu Wu, Yi Zhang, Guidong Zhang, Zheng Yang, and Yunhao Liu. Widar2. 0: Passive human tracking with a single wi-fi link. In *Proceedings of the 16th annual international conference on mobile systems, applications, and services*, pages 350–361, 2018.

[49] Beibei Wang, Qinyi Xu, Chen Chen, Feng Zhang, and KJ Ray Liu. The promise of radio analytics: A future paradigm of wireless positioning, tracking, and sensing. *IEEE Signal Processing Magazine*, 35(3):59–80, 2018.

[50] Zhengxiong Li, Fenglong Ma, Aditya Singh Rathore, Zhuolin Yang, Baicheng Chen, Lu Su, and Wenyao Xu. Wavespy: Remote and through-wall screen attack via mmwave sensing. In *2020 IEEE Symposium on Security and Privacy (SP)*, pages 217–232. IEEE, 2020.

[51] Fahim Niaz, Jian Zhang, Muhammad Khalid, Kashif Naseer Qureshi, Yang Zheng, Muhammad Younas, and Naveed Imran. Ai enabled: a novel iot-based fake currency detection using millimeter wave (mmwave) sensor. *Computing*, 106(8):2851–2873, 2024.

[52] Kumar Vijay Mishra, MR Bhavani Shankar, Visa Koivunen, Bjorn Ottersten, and Sergiy A Vorobyov. Toward millimeter-wave joint radar communications: A signal processing perspective. *IEEE Signal Processing Magazine*, 36(5):100–114, 2019.

[53] Zhengxiong Li, Baicheng Chen, Xingyu Chen, Huining Li, Chenhan Xu, Feng Lin, Chris Xiaoxuan Lu, Kui Ren, and Wenyao Xu. Spiralspy: Exploring a stealthy and practical covert channel to attack air-gapped computing devices via mmwave sensing. In *The 29th Network and Distributed System Security (NDSS) Symposium 2022*. The Internet Society, 2022.

[54] Qualcomm rolls out chips for 802.11a, 2018. Available at: https://www.eetimes.com/document.asp?doc_id=1333870.

[55] Iwr1443 single-chip 76- to 81-ghz mmwave sensor evaluation module, 2021. Available at: https://www.ti.com/tool/IWR1443BOOST.

[56] Chenshu Wu, Feng Zhang, Beibei Wang, and KJ Ray Liu. mmtrack: Passive multi-person localization using commodity millimeter wave radio. In *IEEE INFOCOM 2020-IEEE Conference on Computer Communications*, pages 2400–2409. IEEE, 2020.

[57] Retail counterfeit detection, 2024. Available at: https://www.retailitinsights.com/doc/retail-counterfeit-detection-0002.

[58] Counterfeit detection machine, 2024. Available at: https://www.shopstuff.co.uk/acatalog/Glory-UW500.html.

[59] Cassida 5520 uv/mg money counter, 2024. Available at: https://cassidausa.com/5520-series-currency-counter.

[60] Iwr1443 dca1000evm, 2021. Available at: https://www.ti.com/tool/DCA1000EVM.

[61] Meera Moydeen Abdul Hameed and Badr M Thamer. Preparation of persistently luminescent polyacrylic acid-based nanocomposite ink for secure encoding. *Journal of Photochemistry and Photobiology A: Chemistry*, 448:115319, 2024.

[62] Chengkun Jiang, Junchen Guo, Yuan He, Meng Jin, Shuai Li, and Yunhao Liu. mmvib: micrometer-level vibration measurement with mmwave radar. In *Proceedings of the 26th Annual International Conference on Mobile Computing and Networking*, pages 1–13, 2020.

[63] Luyao Liu, Wendong Xiao, Jiankang Wu, and Shenglang Xiao. Wavelet analysis based noncontact vital signal measurements using mm-wave radar. In *Green, Pervasive, and Cloud Computing: 15th International Conference, GPC 2020, Xi'an, China, November 13–15, 2020, Proceedings 15*, pages 3–14. Springer, 2020.

[64] Dominik Łuczak. Mechanical vibrations analysis in direct drive using cwt with complex morlet wavelet. *Power Electronics and Drives*, 8(1):65–73, 2023.

[65] Shuhao Cui, Xuan Jin, Shuhui Wang, Yuan He, and Qingming Huang. Heuristic domain adaptation. *Advances in Neural Information Processing Systems*, 33:7571–7583, 2020.

[66] Kaiming He, Xiangyu Zhang, Shaoqing Ren, and Jian Sun. Deep residual learning for image recognition. In *Proceedings of the IEEE conference on computer vision and pattern recognition*, pages 770–778, 2016.

[67] Mohammed Mahbubur Rahman, Sevgi Z Gurbuz, and Moeness G Amin. Physics-aware generative adversarial networks for radar-based human activity recognition. *IEEE Transactions on Aerospace and Electronic Systems*, 2022.